Applied Geochemistry 44 (2014) 111–120

Contents lists available at ScienceDirect

Applied Geochemistry

journal homepage: www.elsevier.com/locate/apgeochem

Study of an aplite dyke from the Beira uraniferous province in Fornos de Algodres area (Central Portugal): Trace elements distribution and evaluation of natural radionuclides

Maria José Trindade [a,c,*], Maria Isabel Prudêncio [a,c], Christopher Ian Burbidge [a,c], Maria Isabel Dias [a,c], Guilherme Cardoso [a,c], Rosa Marques [a,c], Fernando Rocha [b,c]

[a] Campus Tecnológico e Nuclear, Instituto Superior Técnico (CTN/IST), Universidade Técnica de Lisboa, EN10 (km 139.7), 2695-066 Bobadela LRS, Portugal
[b] Departamento de Geociências, Universidade de Aveiro, Campus Universitário de Santiago, 3810-193 Aveiro, Portugal
[c] GeoBioTec Research Centre, Universidade de Aveiro, Portugal

ARTICLE INFO

Article history:
Available online 9 August 2013

ABSTRACT

A uranium-rich aplite dyke with spheroidal alteration sited in the Beira uraniferous province, in Fornos de Algodres area (Northern Central Portugal) was studied, focusing on trace element distributions, especially U, in the aplite. A vertical profile, different size fractions, and various concentrically weathered layers of rock, were examined. The main goal of the work is to better understand the geochemical behavior and distribution of natural radionuclides in fine-grained granitic rocks, and changes that occur during weathering. The rock samples obtained from this site were examined using chemical and mineralogical methods: instrumental neutron activation analysis (INAA) and the X-ray diffraction (XRD). Field gamma spectrometry (FGS) and high resolution gamma spectrometry (HRGS) in the laboratory were also performed in order to determine concentrations of the natural radionuclides (K, Th and U) responsible for terrestrial gamma radiation, and for comparison of results with INAA measurements, enabling some information concerning radon losses.

The U concentration in the studied samples vary between 4.5 and 83 ppm (always higher than upper continental crust value), with the higher values detected in the clay and sand fractions of weathered aplite (residual clay) and in the rounded boulders of aplite with spheroidal weathering, especially in the core. Strong variations in natural radionuclide contents, especially observed between residual clay and soil, relate to differences in source material. The large difference between pre-Rn and post-Rn values obtained by HRGS suggests high loss of radon (40% minimum), which is in accordance with field measurements. Due to generally high concentration of U, the aplite is a potentially strong source of emission of radon to the atmosphere with consequent radiological hazards.

1. Introduction

Long-lived radionuclides, like uranium and thorium, and their decay products emit ionizing radiation to the atmosphere that under certain conditions can reach hazardous radiological levels and represent a potential risk to human health (Singh et al., 2009). Most harmful radionuclide contamination comes from human activities, through the mining and processing of ores, combustion of fossil fuels and application of phosphate fertilizers, for example. The naturally occurring radionuclides (K, Th and U) are present in rock forming minerals and soils in variable concentrations, which in general are not a concern to the environment or human health (Elles and Lee, 2002); however, there are areas with relatively high natural concentrations of these elements due to their geological context. Because the general population is exposed mainly to terrestrial radiation of natural origin (UNSCEAR, 1988), it is important to study the background natural radioactivity levels (coming mainly from ^{238}U, ^{232}Th and ^{40}K) in rocks and soils to assess the gamma radiation dose for the population and to have a baseline for future changes in the environmental radioactivity due to human activities (Singh et al., 2009).

The Central Iberian Zone contains U–Ra metallogenic deposits in a significant uraniferous metallogenic province (Beira Uraniferous Province), which has been exploited since the beginning of the 20th century, until recently (Carvalho et al., 2007). The uranium mineralization is related with late tectonic and metallogenetic phenomena that have affected the post-tectonic Hercynian granitic batholiths (Azevedo and Nolan, 1998). In the Beiras region, the granite belonging to calc-alkaline series is generally heavily fractured, particularly the NNE–SSW to ENE–WSW and NNW–SSE

* Corresponding author at: Campus Tecnológico e Nuclear, Instituto Superior Técnico (CTN/IST), Universidade Técnica de Lisboa, EN10 (km 139.7), 2695-066 Bobadela LRS, Portugal. Tel.: +351 21 9946215; fax: +351 21 9946185.
E-mail address: mjtrindade@ctn.ist.utl.pt (M.J. Trindade).

0883-2927/$ - see front matter © 2013 Elsevier Ltd. All rights reserved.
http://dx.doi.org/10.1016/j.apgeochem.2013.07.024

to NW–SE systems (Goinhas, 1987) and is frequently intersected by dykes of basic or felsic rock. In this region, the intra-granitic uranium bearing veins can be any of the following types: jasperized veins, quartz veins, basic rock veins and granitic breccia, sometimes with limonite. Other mineral occurrences essentially consist of secondary uranium minerals (Gusmão, 2008).

The granitic rocks and associated dykes from Fornos de Algodres area commonly have higher U and Th concentrations when compared to most granitoids of the country (average U values of 6.7–8.9 ppm, Neves et al., 1996), and this makes the area ideal for the study of the distribution of these elements during weathering. The U contents in the Beiras granites were estimated between 7 and 22 ppm (Salgado et al., 1998), whereas in dykes and fault zones even higher U values have been detected (15–223 ppm, Salgado et al., 1998) associated to an anomalous radiometric background.

The present work focused on the trace element distributions, especially of natural radionuclides, in an aplite dyke that intersects the most abundant granite type of the studied area. A vertical profile, different size fractions, and various concentrically weathered shells of aplite rock were examined. The goal is to better understand the geochemical behavior and redistribution of radionuclides, especially U, during weathering of these rocks considering the objectives of ascertain their background levels in rocks and soils, their vertical distribution, their fractionation with particle size and the main processes responsible for their mobility.

2. Geological context

The majority of granitic rocks from the Northern Iberian Hercynian massif are correlated with the third deformation phase (D3) of the Variscan continent–continent collision that took place during Late Devonian to Carboniferous times (Ribeiro et al., 1983; Matte, 1986). In the Fornos de Algodres area most granitic rocks are discordant, intrusive, late-post-kinematic plutons (315–270 Ma) (Ferreira et al., 1987; Pinto et al., 1987), and a minority are small bodies of deformed syn-D3 granitoids (340–320 Ma). The whole batholith was emplaced into metasedimentary rocks of Precambrian–Cambrian to Lower Ordovician age from which only small bodies can be seen in the area (Fig. 1). These metasedimentary rocks were strongly affected by Variscan deformation phases and late-stage activity related to subvertical shearing and faulting (Azevedo and Nolan, 1998), giving origin to the emplacement of dolerite and aplite–pegmatite veins.

In the area comprising Fornos de Algodres and Celorico da Beira, the porphyroid monzonitic granite is volumetrically the most important lithological type presently exposed, outcropping as a large, irregularly shaped pluton, which is crosscut by smaller bodies of granitoids with variable composition, grain size and textures. Its major rock-forming minerals are quartz, plagioclase, K-feldspar, biotite and muscovite and as accessory phases has commonly apatite, monazite, zircon and ilmenite (Azevedo and Nolan, 1998).

3. Materials

The focus of this research is a strongly weathered aplite dyke, with relatively high uranium content, intruded into coarse- to medium-grained porphyroid monzonite two-mica granite ("Granito da Muxagata" in *Carta Geológica de Portugal,Folha 17-B*, Gonçalves et al., 1990), and located near Aldeia Nova, in Fornos de Algodres area, within the Beira uraniferous province (Fig. 1). Five samples, three residual clays (FQC0, FQC1 and FQC2) and two soils (S2FQC and S1FQC), were collected along a vertical profile in the

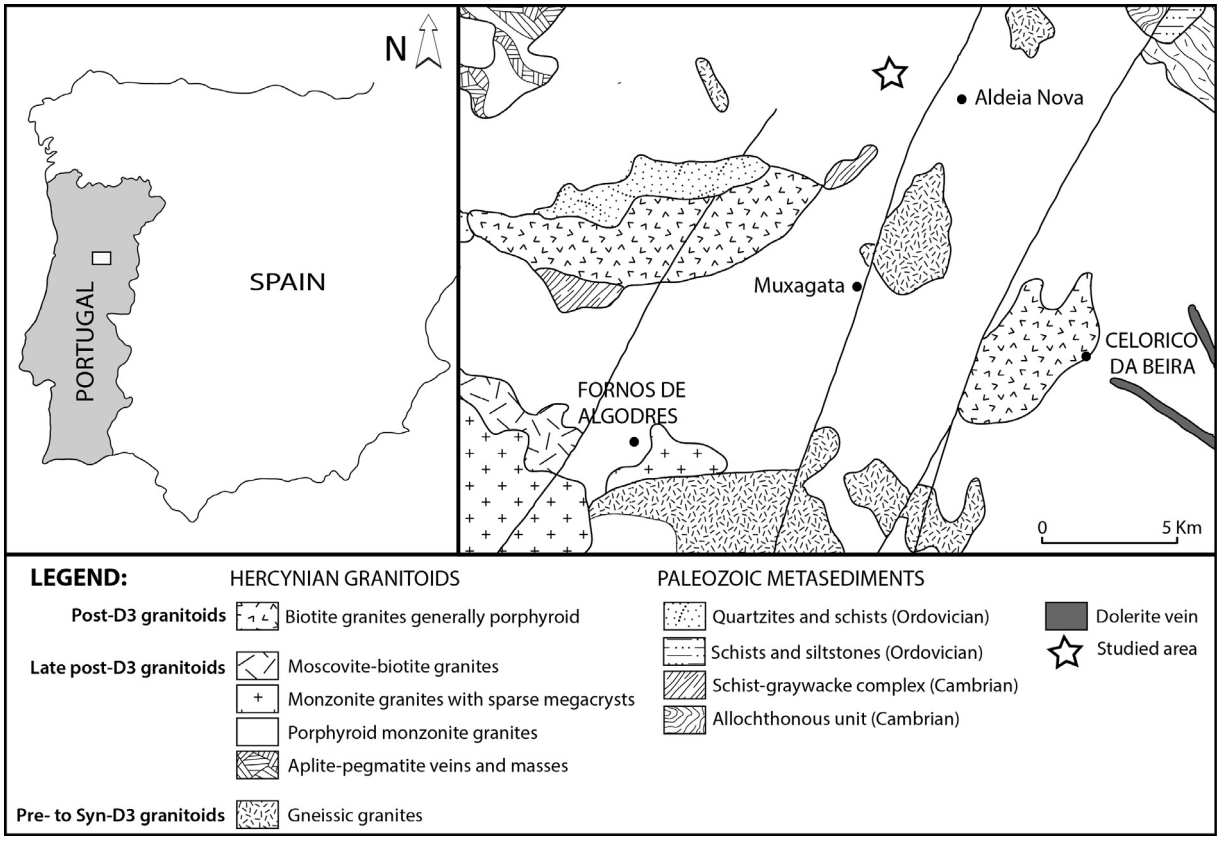

Fig. 1. Geological sketch map of the Fornos de Algodres area (Northern Central Portugal). Drawing based on the digital *Carta Geológica de Portugal*, *1:500,000*, from the geoPortal LNEG (http://geoportal.lneg.pt/geoportal/mapas/index.html).

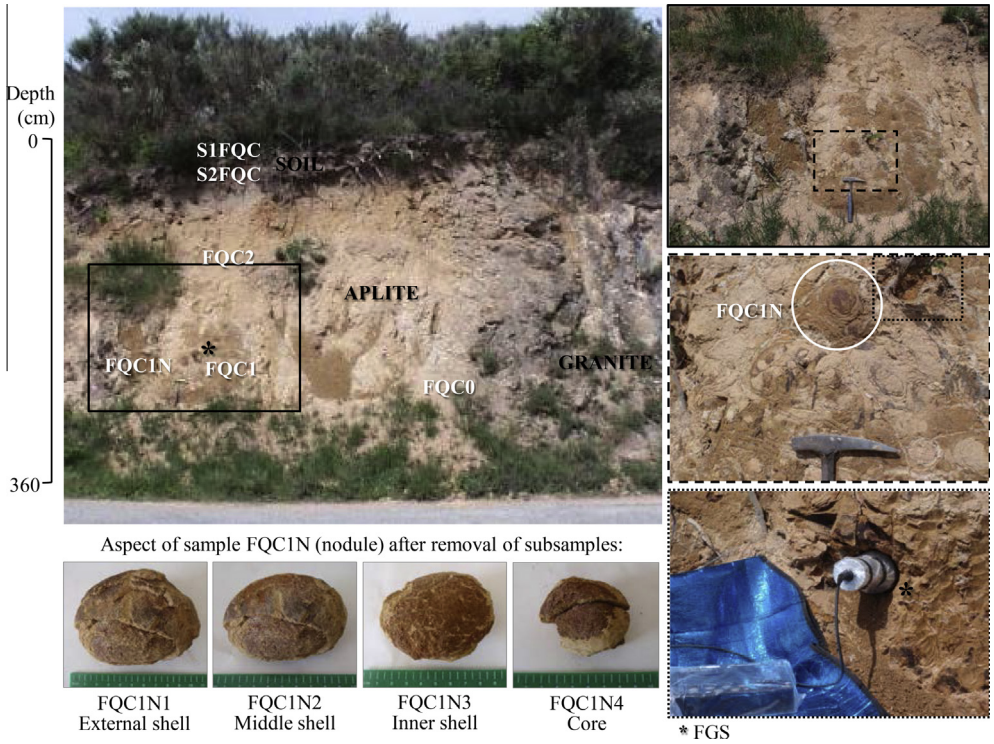

Fig. 2. Outcrop of the aplite dyke studied, with indications of sampling locations and field gamma spectrometry (FGS) measurement.

aplite dyke, in order to analyze the distribution of U and other major and trace elements in a weathering profile (Fig. 2). As the aplite presents advanced spheroidal weathering, consisting of yellowish residual clay with boulders of less altered rock, it offers a good opportunity to study in detail the elemental mobilization and redistribution during this localized weathering process. Therefore, for one nodule (FQC1N) of about 10 cm long was collected in the same place as sample FQC1. Various sub-samples were considered corresponding to the core (FQC1N4) and three shells of progressively more decayed material (inner shell – FQC1N3, middle shell – FQC1N2, and external shell – FQC1N1).

In order to study in more detail the distribution of the naturally occurring radionuclides and other trace elements in the aplite, we took into account their distribution by grain size, which is a fundamental characteristic of sediments that greatly influences the environmental mobility of radionuclides. For two soil samples (S1FQC and S2FQC) and two residual clays (FQC1 and FQC2), in addition to the whole rock analysis, we made grain-size separation and studied the various fractions (sand: >63 μm, coarse silt: 20–63 μm, fine silt: 2–20 μm and clay: <2 μm).

Some information on the geochemistry and mineralogy of weathered aplite from Fornos de Algodres region can be found in Dias et al. (2000), Trindade et al. (2010) and Trindade et al. (2011).

4. Methods

Whole rock samples of weathered aplite and the various grain-sized fractions were analyzed both in the mineralogical and chemical point of view. The >2 mm fragments were separated by dry sieving and not considered for analysis. Total samples (<2 mm) were crushed into a fine powder using an agate mortar and then homogenized. The >63 μm size fraction was obtained by wet sieving, using ASTM standard sieves; finer fractions (20–63 μm, 2–20 μm and <2 μm) were obtained by sedimentation according to Stokes law, undertaken on hexametaphosphate dispersed suspension and considering adequate times of rest before siphoning the first 10 centimeters of suspension. Oriented slides of the clay fraction (<2 μm) were prepared by placing the suspension on a thin glass plate and air-dried.

The mineralogical composition was obtained by X-ray diffraction (XRD), using a Philips X'Pert Pro diffractometer, with a PW 3050/6x goniometer, Cu Kα radiation, and fixed divergence slit, operating at 45 kV and 40 mA. The powdered samples were prepared as non-oriented aggregates and used to obtain diffraction patterns. Scans were run from 4° to 60° 2θ, using a step size of 0.02° 2θ and a scan step time of 2 s. The identification of clay minerals was performed on oriented <2 μm fraction (untreated and after ethylene-glycol solvation at 80 °C and heating to 550 °C during 2 h) in the 4° to 20° 2θ range, using 0.5° divergence slit and the same conditions as previously.

Identification of crystalline phases by XRD was carried out using the International Centre for Diffraction Data Powder Diffraction Files (ICDD PDF). The estimation of mineral abundances was done by measuring the diagnostic peak area, considering the full width at half maximum (FWHM), of each mineral and then weighted by empirically estimated factors (reflection powers) (Schultz, 1964; Biscaye, 1965; Martin-Pozas, 1968; Galhano et al., 1999; Oliveira et al., 2002) according to criteria recommended by Schultz (1964) and Thorez (1976). The diagnostic peaks used and the corresponding reflection powers (in parenthesis) were the following: quartz – 3.35 Å (2), phyllosilicates – 4.46 (0.1), alkali feldspar – 3.25 Å (1), plagioclase – 3.20 Å (1), anatase (1), hematite – 2.70 (1.3), illite – 10 Å (0.5), kaolinite – 7 Å (1), vermiculite – 14 Å (3), gibbsite – 4.85 Å (1) and smectite – 14 Å (4). Given the uncertainties involved in the semi-quantitative method, the results should only be taken as rough estimates of mineral percentages. The amount of phyllosilicates was estimated measuring the 4.48 Å peak areas on the whole rock XRD pattern. The percentage of minerals in the <2 μm fraction was estimated by measuring the peak areas on the glycolated oriented mounts.

The chemical composition was determined by instrumental neutron activation analysis (INAA), using the Portuguese Research Reactor at CTN/IST. For the analysis, samples were previously crushed, using an agate mortar, and homogenized, then dried in an oven at 110 °C for 24 h. After thermal treatment the samples were put in a desiccator for cooling for 2 h, and then about 200–300 mg were weighed in cleaned high-density polyethylene vials, as well as two multi-elemental reference materials (GSD-9 and GSS-1) from the Institute of Geophysical and Geochemical Prospecting (IGGE). Long irradiations (7 h) were performed in the core grid of the reactor at a thermal flux of 4.4×10^{12} $n\ cm^{-2}\ s^{-1}$; $\varphi_{epi}/\varphi_{th} = 1.4\%$; $\varphi_{th}/\varphi_{fast} = 12.1$. Two γ-ray spectrometers were used: one consisting of a 150 cm^3 coaxial Ge detector and another consisting of a low energy photon detector (LEPD), both connected through Canberra 2020 amplifiers to Accuspec B (Canberra) multichannel analyzers. Different delay times were selected to determine radionuclides with different half-lives. After 4-day decay, the samples were counted in the detectors to measure medium-lived elements: Na, K, Ga, As, Br, La, W, Sm and U. Following additional 4-week decay, the samples were counted again, yielding the measurement of the following long-lived elements: Fe, Sc, Cr, Co, Zn, Rb, Sb, Cs, Ba, Zr, Ce, Nd, Eu, Tb, Yb, Lu, Hf, Ta and Th. Details concerning the measurement and processing of the gamma spectra can be found in Gouveia and Prudêncio (2000) and Dias and Prudêncio (2007). The relative precision and accuracy of the method are, in general, to within 5%, and occasionally within 10%.

Within the U and Th series, isotopes of gaseous Rn and soluble U and Ra may escape a porous sample matrix, leading to disequilibrium in the decay chains (Murray and Aitken, 1988; Guibert et al., 2009; Reis, 2007). Field gamma-ray spectrometry (FGS) was undertaken in situ for comparative assessment of the spatial distribution and equilibrium conditions of daughter radionuclides, relative to INAA data for the parent concentrations, and so to facilitate assessment of certain environmental hazards such as radon loss (Pereira et al., 2010). For a selected sample (FQC1) of aplite the apparent concentrations of the parent elements K, Th and U were evaluated by high resolution gamma spectrometry (HRGS) of inactivated sample material, to permit a more detailed comparison with INAA data.

The geochemical variability in the vertical profile of aplite dyke was assessed through normalization of each sample relative to the deeper less altered sample (FQC0) of the profile. The difference in chemical composition of the various shells and core of the nodule were analyzed after normalizing each subsample relative to the nodule's core (FQC1N4). Finally, the chemical variability among different grain-size fractions of three samples collected at various heights of the profile was observed after normalization of each size fraction relative to the respective whole sample. All geochemical data were previously normalized in relation to scandium, since the normalization of elemental concentrations to an immobile, conservative, element like Sc provides deeper insights about the distribution of other elements than consideration of the absolute concentration alone (Dias and Prudêncio, 2008).

FGS measurements were conducted in situ at the point of sampling, using a 3″ × 3″ NaI(TL) probe with a HPI Rainbow MCA. Stripped counts in the windows 1380–1530 keV, 1690–1840 keV, and 2550–2760 keV (designed to obtain signals dominated by ^{40}K, ^{214}Bi and ^{208}Tl respectively), were calibrated relative to previous measurements in the Oxford and the Gif-sur-Yvette blocks (Richter et al., 2003), to obtain apparent parent element concentrations, assuming equilibrium in the ^{232}Th and ^{238}U series.

HRGS of non-activated material in the laboratory was performed for sample FQC1 for 12 h, using a 40% efficiency cooled HPGe detector in a low activity lead castle. 85 g of un-milled sample in a polyurethane container was sealed and rested for several months prior to measurement. To calculate apparent parent radionuclide concentrations, background subtracted count-rates were compared with those from powder of the geo-reference sample GSD9 (sediment) in a similar container (parent element concentrations from Govindaraju, 1994). ROIs were used from 19 emission

Table 1
Mineralogical composition (given in percentages) of studied samples from the aplite dyke, obtained by semi-quantification based on XRD data.

Description		Sample	Non-oriented whole rock					Oriented < 2 μm fraction				
			Qtz	Phy	kF	Pl	Ant	I	K	V	G	S
Profile	Soil	S1FQC	32	18	27	23	0					
	Soil	S2FQC	35	21	27	17	0					
	Weathered aplite	FQC2	13	71	11	0	5					
	Weathered aplite	FQC1	6	70	16	0	8					
	Weathered aplite	FQC0	12	45	36	0	7					
Nodule	External shell	FQC1N1	7	77	9	0	7					
	Middle shell	FQC1N2	6	70	15	0	9					
	Inner shell	FQC1N3	6	72	13	0	9					
	Core	FQC1N4	7	67	15	0	11					
Size fractions	>63 μm	S1FQC	42	4	34	20	0					
	20–63 μm		6	19	17	58	0					
	2–20 μm		11	76	5	8	0					
	<2 μm		4	90	3	3	0	47	31	7	15	0
	>63 μm	S2FQC	36	3	44	17	0					
	20–63 μm		17	44	11	28	0					
	2–20 μm		6	75	11	8	0					
	<2 μm		4	91	2	3	0	27	47	13	13	0
	>63 μm	FQC2	47	39	8	0	6					
	20–63 μm		15	66	14	0	5					
	2–20 μm		7	84	6	0	3					
	<2 μm		4	89	3	0	4	12	85	0	0	3
	>63 μm	FQC1	34	47	8	0	11					
	20–63 μm		8	70	15	0	7					
	2–20 μm		4	71	20	0	5					
	<2 μm		2	77	12	0	9	20	40	40	0	0

Qtz – quartz; Phy – phyllosilicates; kF – potassium feldspar; Pl – plagioclase; Ant – anatase; I – illite; K – kaolinite; V – vermiculite; G – gibbsite; S – smectite.

peaks of the isotopes ^{40}K, ^{234}Th, ^{226}Ra ($+^{235}U$), ^{214}Pb, ^{214}Bi, ^{210}Pb, ^{228}Ac, ^{224}Ra, ^{212}Pb, ^{212}Bi, ^{208}Tl. Averages were calculated for each isotope, for pre- and post-radon isotopes in the ^{238}U series, and for the total ^{238}U and ^{232}Th series' assuming equilibrium. The combination of INAA, HRGS and FGS measurements enables inferences related to dosimetric homogeneity and as parent element concentrations are compared with apparent concentrations based on pre- and post- radon emissions it can help detect disequilibrium in the U series, including radon emission.

5. Results and discussion

5.1. Mineralogy

The mineralogical composition of the whole rock and clay fraction of the studied samples is presented in Table 1. In general samples have similar compositions, with varying proportions of the different minerals. They are mainly composed of quartz, phyllosilicates, K-feldspar, plagioclase and anatase; the clay minerals consist of vermiculite, kaolinite, illite and less frequently gibbsite and smectite. However, some mineralogical particularities can be enhanced as follows: (i) in the vertical profile it is evident that soils are richer in quartz and poorer in phyllosilicates than weathered aplite, and contain plagioclase but not anatase; the clay minerals found in the soils are kaolinite and illite in similar proportions and minor vermiculite and gibbsite, whereas in weathered aplite samples kaolinite clearly predominates over illite, being accompanied by abundant vermiculite in sample FQC1 and by small amounts of smectite in sample FQC2 (Fig. 3); (ii) in the studied nodule the proportion of clay minerals tends to increase towards the external shell, but this is a very small increase, regarding that the method used to quantify XRD results is not very precise. Although the abundance of clay minerals was not determined in diffractograms of oriented mounts, the intensity of 14 Å and 7 Å peaks in whole rock diffractograms suggests increasing kaolinite/vermiculite ratio in the same sense; and (iii) considering the distribution of minerals by size fraction, the amount of quartz decreases whereas the amount of phyllosilicates increases greatly with decreasing grain-size, as expected. Feldspar appears to have the same trend as quartz in soils but not in the weathered aplite.

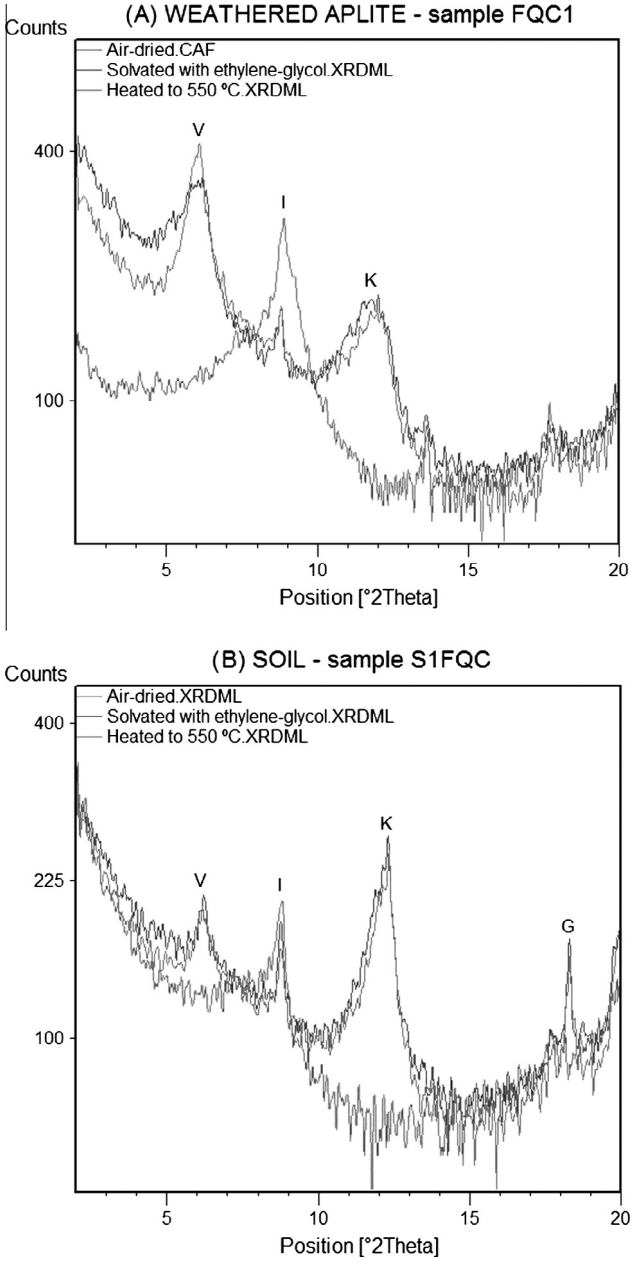

Fig. 3. X-ray oriented (<2 μm fraction) diffractograms (air-dried, glycolated and heated) for a residual clay (A) and a soil (B) along a vertical profile in the aplite. Abbreviations: G – gibbsite, I – illite, K – kaolinite, V – vermiculite.

5.2. Geochemistry: INAA results

5.2.1. Distribution of trace and rare earth elements

5.2.1.1. Vertical profile. Comparison of aplite residual clays (FQC1 and FQC2) with the deeper aplite sample (FQC0) show similar concentrations for most elements, although a slight enrichment in Na, Fe, Co, Cs and rare earth elements (REEs) and depletion in K, Rb and Zr can be observed (Fig. 4). The composition of soils is quite different from the residual clays beneath; they have higher concentrations of Th and alkali metals, especially Na, and lower amounts of some REE and U. Such a distinct chemical composition between clay and soil samples from the same vertical profile is in accordance with the mineralogy (higher amounts of quartz and feldspars and lower amounts of phyllosilicates in soils) and suggests that the soils were not fully developed in situ; abundant detrital components came probably from a different weathered source area, most likely granites (Trindade et al., 2013). Thus, it is plausible to consider the effect of colluviation/slopewash in the development of the soils.

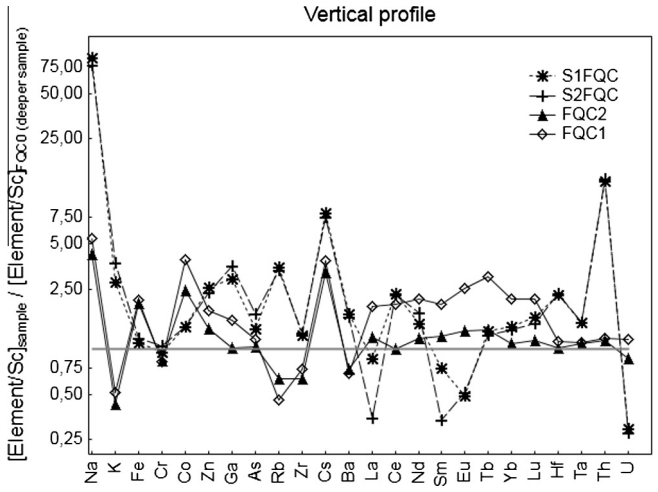

Fig. 4. Enrichment factors of chemical elements, normalized to Sc, in sediments along the vertical profile compared to the respective deeper level.

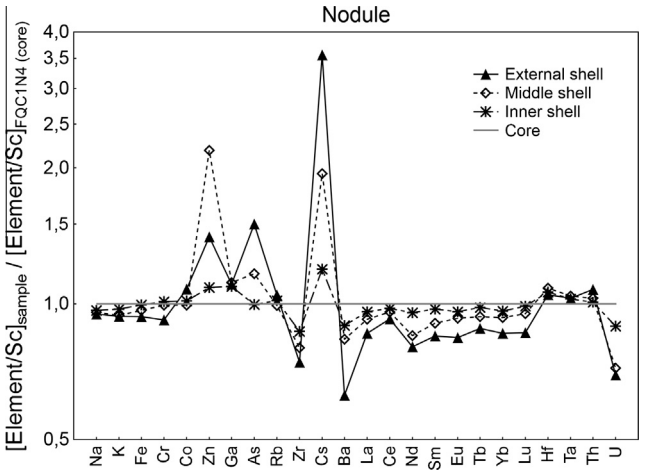

Fig. 5. Enrichment factors of chemical elements, normalized to Sc, in the nodule shells compared to the respective core.

5.2.1.2. Nodule. The aplite nodule shows accentuated enrichment of Cs, Zn and As in the two more external/altered shells (Fig. 5), suggesting that these elements were mobilized from the degraded primary minerals of aplite, redistributed and included in the alteration products, or they were brought by the fluids to the rock zones being altered, where they precipitated together with the alteration materials. On the contrary, the more external shells of the nodule show some depletion in Ba, Zr, U, REE, Na, K, Fe and Cr, indicating these elements are being solubilized and removed from the weathered aplite. Chondrite normalized REE patterns of the various shells and core are similar, being characterized by fractionation between light and heavy REE and by negative Ce and Eu anomalies, as is typical of felsic rocks.

5.2.1.3. Grain-size fractions. Considering the compositional variations between different size fractions of residual clay samples in respect to the whole rock, it is clear that the clay fraction is enriched in REE and Th, as well as in Zr and Ba in sample FQC1, and depleted in alkalis, mainly Na and K (Fig. 6). The fine silt fraction tends to be the most depleted in REEs and the sand fraction tends to be the most enriched in Cr, As, Cs and U. The clay and fine silt fractions of the soils are characterized by lower Na, K, Rb, Ba, Zr, Yb, Lu, Hf and Ta contents and higher Cr, Co, As, La, Sm and U contents than the whole rock (Fig. 7). The 20–63 μm fractions are especially enriched in Zr, Hf, and REE, with the exception of Eu. The sand fraction has the most similar composition to the whole rock; the main differences are the enrichment in U in both samples, and also of Ga and As in sample S1FQC as well as depletion in Zr.

5.2.2. Distribution of natural radionuclides (K, Th and U)

5.2.2.1. Vertical profile. With respect to the distribution of naturally occurring radionuclides (K, Th and U) through the weathering profile, the much higher concentration of Th and K in soils relative to weathered aplite is most likely related to the abundance of feldspars and the presence of monazite-type phases, which are frequent in the granite of this region. Potassium content clearly decreases in the more superficial samples of residual clay, whereas Th tends to increase slightly. Uranium is much enriched in the studied samples relative to Upper Continental Crust, especially in weathered aplite where the U/Sc ratio is 14–19 times UCC (Fig. 8); the variation of U in residual clays does not follow a linear trend.

The observed differences are consistent with the three radionuclides following different pathways of evolution during the

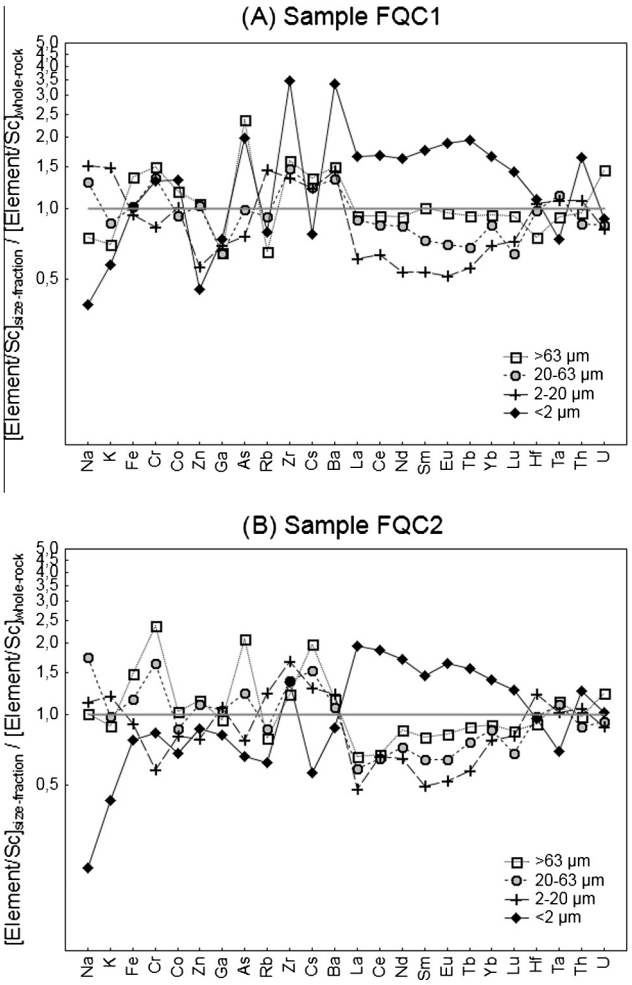

Fig. 6. Enrichment factors of chemical elements, normalized to Sc, in different grain-size fractions compared to the respective whole-rocks of residual clays: (A) sample FQC1 and (B) sample FQC2.

alteration of granitic rocks (Perrin et al., 2006). The K cations are leached during decomposition of K-bearing minerals, like feldspars and micas, and clay minerals depleted in K are formed; therefore, K content declines gradually with an increasing degree of weathering (e.g. Taboada et al., 2006). The contents of U and Th do not show a similar trend of variation, suggesting the presence of more complex processes controlling their concentration in the weathering process (Chan et al., 2007). There is a general lack of mobility of Th in the weathered igneous rocks, it is generally removed by settling of particles from the weathering solution, which mix with sediment grains (Hall and McCave, 2000) and produce surface coatings enriched in Th (Reynolds et al., 2003). In this way, a slight increase of Th commonly accompanies increased weathering of aplite. The removal of U from the host rock is mainly through the dissolution of uranyl compounds in the presence of groundwater; the mobility of uranyl ions depends on several parameters, such as the alkalinity of the groundwater, the redox potential and the presence of complexing agents in the groundwater (e.g. Porcelli and Swarzenski, 2003). Most non-minerallic U and Th reside in the Fe-oxides and clay minerals in the weathered rock by adsorption (Abdelouas et al., 2000).

5.2.2.2. Nodule. Thorium content in the studied nodule is lower than Upper Continental Crust, while K has similar concentrations. Both element concentrations are similar for the diverse shells

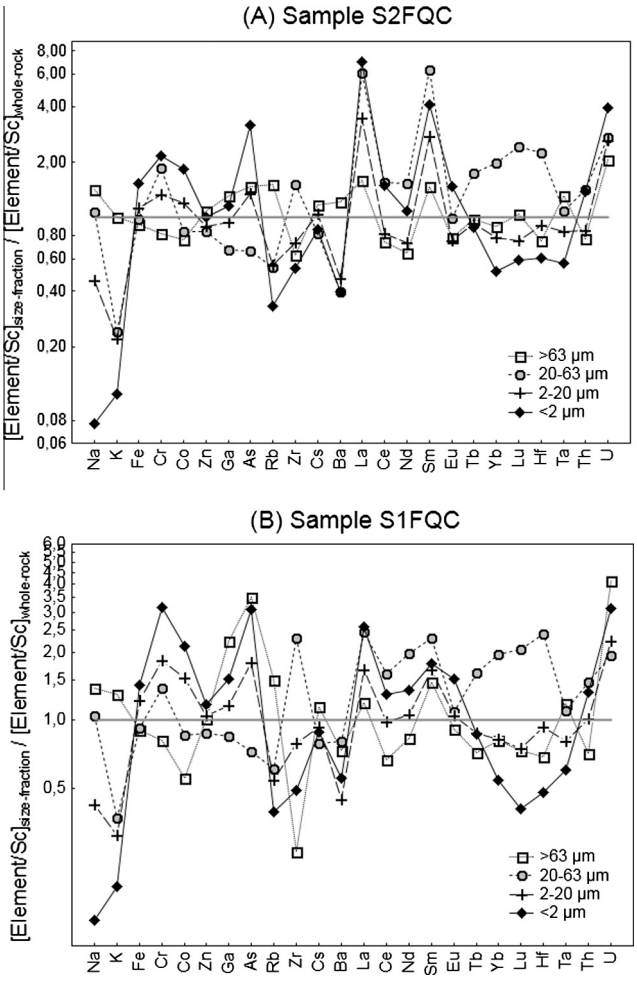

Fig. 7. Enrichment factors of chemical elements, normalized to Sc, in different grain-size fractions compared to the respective whole-rock of the soils: (A) sample S1FQC and (B) sample S2FQC.

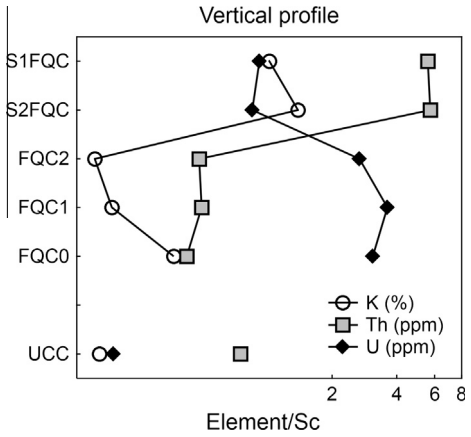

Fig. 8. Distribution of K, Th and U along the vertical profile. The upper continental crustal (UCC) values (Rudnick and Gao, 2003) are given for comparison.

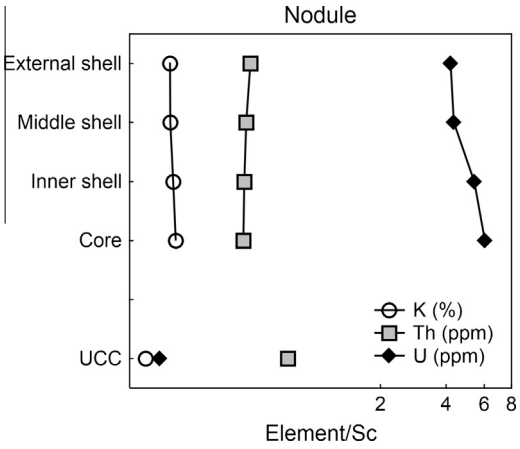

Fig. 9. Distribution of K, Th and U across the aplite nodule.

and core of the nodule. Uranium is clearly enriched in the nodule (U/Sc = 22–31 times UCC), especially in the core, with slightly decreasing U contents towards the more weathered external shell (Fig. 9).

5.2.2.3. Grain-size fractions. In the residual clays resulting from weathering of aplite, some patterns with grain-size fraction were consistent for the two samples studied (Fig. 10). The K content varies around the UCC value. It increased with decreasing grain size, from sand to fine silt, but decreased considerably in the clay fraction. Thorium content was generally lower than UCC and tended to increase in the finer fractions. The U concentration in all fractions was much higher than UCC (U/Sc = 12–27 times UCC) and tended to be higher in clay and sand fractions. Both U and especially Th enrichment in the clay minerals of weathered granitic rocks have been previously reported (e.g. Taboada et al., 2006). Radionuclide concentration tends to increase with decreasing particle-size because they are mostly concentrated in the surface of the particles (Baeza et al., 1995). Therefore, the weathering of granitic rocks may increase the environmental risk, but at the present site the accumulation of soil with different provenance, and characterized by much lower U contents, limits to some extent the redistribution and transfer of these radioactive elements.

The studied soils show great variations in K content in different size fractions of a sample. Values were much higher than Upper Continental Crust for the sand fraction (K/Sc ≈ 8 times UCC), decreasing to approximate UCC concentrations in clay fraction (Fig. 11). They have remarkably high Th contents (Th/Sc = 5–11 times UCC); Th tends to increase slightly for smaller grain-sizes but shows enrichment, out of trend, in the 20–63 µm fraction of soils. Uranium is enriched relative to UCC (U/Sc = 9–20 times UCC) but to a lower extent than the residual clays, as seen previously; uranium content tends to be higher in clay and sand fractions of sample S1FQC, as was observed for residual clays, but is depleted in the >63 µm fraction of the other sample.

U migration and hence disequilibrium in the U series may be indicated by the heterogeneous distribution of U concentrations in the studied aplite (Woodborne and Vogel, 1997), and by Th/U ratios of approximately 0.14: ca. 50% those expected based on average sediment or UCC composition (Murray and Aitken, 1988; Rudnick and Gao, 2003). These observations may also result from dilution effects and enrichment in Th, respectively. To better test for disequilibrium, high resolution gamma spectra were used in this work. A thorough understanding of the distribution and migration of the radionuclides in the weathering process, as described above, is critically important for the interpretation of gamma-ray spectrometry data.

5.3. Natural radionuclides concentrations – methods comparison

For one residual clay of aplite (sample FQC1), data on the concentration of naturally occurring radionuclides were obtained

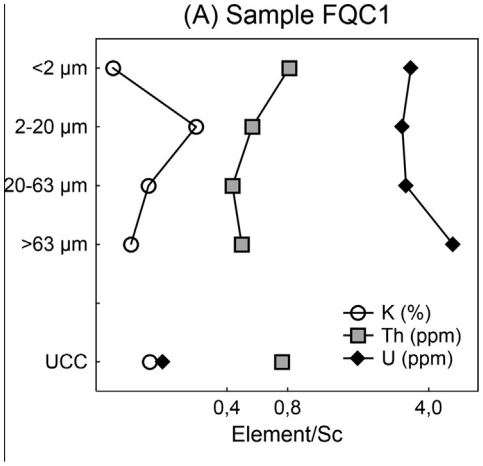

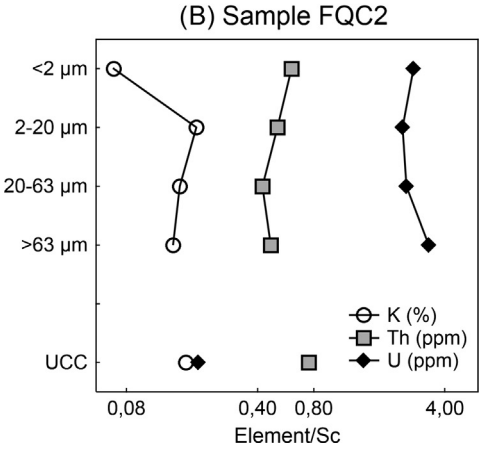

Fig. 10. Distribution of K, Th and U in various grain-size fractions of the residual clays: (A) sample FQC1 and (B) sample FQC2. UCC is Upper Continental Crust.

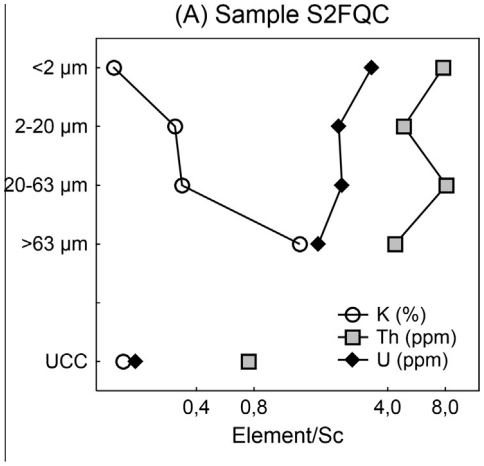

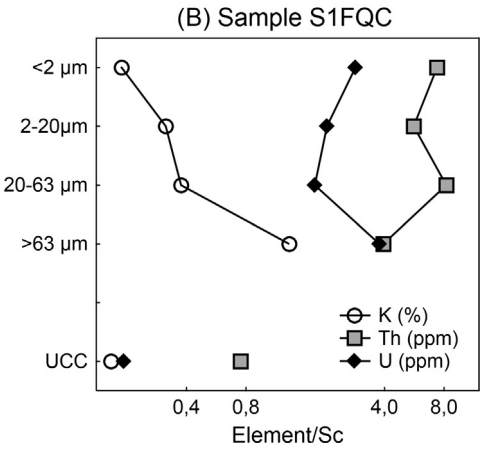

Fig. 11. Distribution of K, Th and U in various grain-size fractions of the soils: (A) sample FQC1 and (B) sample FQC2.

using three complementary methods: (i) instrumental neutron activation analysis (INAA); (ii) field gamma spectrometry (FGS) and (iii) high resolution gamma spectrometry (HRGS in the laboratory). In this way, it is possible to cross-compare data for concentrations of the parent radionuclides and some of their daughters generated by radioactive decay, in field and laboratory conditions. More detailed indications can thus be obtained in relation to disequilibrium in the U and Th decay chains caused by movements of elements in aqueous solution (Carvalho et al., 2007) or the escape of gaseous radon from the porous sample matrix (Pereira et al., 2010), which may have potential harmful radiological impact for the environment or human health.

Apparent parent concentrations are listed in Table 2 for different daughter isotopes in the ^{238}U and ^{232}Th series. These were calculated, assuming equilibrium, from HRGS measurement of the gamma emissions from each isotope, in non-activated, sealed and equilibrated material. The comparison of radionuclides concentrations obtained by using the three methods is presented in Table 3. For INAA, values are the element concentrations, whereas for FGS and HRGS, values are apparent concentrations of parent elements calculated from the activities of different daughters assuming equilibrium: U (post-Rn) for FGS was based on ^{214}Bi emissions, and for HRGS on ^{214}Pb and ^{214}Bi (^{210}Pb was not included), and U (pre-Rn) for HRGS was based on ^{234}Th and ^{226}Ra (+^{235}U) emissions. Taking into account these aspects it is then possible compare the data obtained from the different methods and achieve more complete interpretation.

The K and Th concentrations obtained by INAA, FGS and HRGS are similar. Lower values from the field measurements are thought

Table 2
Apparent parent concentrations (APC) of K, U and Th based on gamma emission from different radionuclides in their decay (series) measured by HRGS.

Isotope	APC[a]	±
^{40}K (%)	3.29	0.12
Series ^{238}U (ppm)		
^{234}Th	35.41	1.32
^{226}Ra (+^{235}U)	35.85	1.87
^{214}Pb	19.52	0.54
^{214}Bi	21.80	2.59
^{210}Pb	23.39	2.14
Series ^{232}Th (ppm)		
^{228}Ac	8.77	0.41
^{212}Pb	9.36	0.27
^{212}Bi	11.48	1.68
^{208}Tl	6.80	0.64

[a] APC: apparent parent concentrations.

Table 3
Parent concentrations and apparent parent concentrations of K, U and Th, measured by INAA, FGS and HRGS. For HRGS, values for U were calculated separately based on emissions from pre- and post-^{222}Rn isotopes, for FGS only post-^{222}Rn emissions were measured.

Element	INAA	FGS	HRGS
K (%)	3.03	2.12	3.29
Th (ppm)	7.91	7.08	8.44
U (parent) (ppm)	57.8	–	–
U (pre-Rn) (ppm)	–	–	35.6
U (post-Rn) (ppm)	–	12.1	21.0

to be related to attenuation of gamma radiation by in situ water. The large difference between parent concentration of U (INAA) and equivalent parent concentration based on pre-radon daughters (HRGS) may indicate systematic effects on U determination. Repeat INAA determinations and comparison of HRGS results with other high activity samples indicates that it does not relate to inhomogeneity, absolute activity levels or self-absorption effects but might relate to the extreme Th/U ratio of this sample, and hence to interference.

The much lower equivalent parent concentrations obtained from post-Rn isotopes, measured in laboratory and field, indicate the significant escape of radon gas. This was not adequately retained by the capsule used in the laboratory (De Corte et al., 2006), or accumulated at its top. However, the interpretation of significant release of radon in the field is supported by the similar value for ^{210}Pb. This has a half-life of 22 years and so indicates radon release through recent decades. The post-/pre-Rn ratio obtained by HRGS measurements represents a minimum for the losses from the sample in its disaggregated state and the post-Rn FGS-/pre-Rn HGRS ratio represents a maximum for the losses in situ: respectively 41% and 66%, or 180 and 290 Bq kg^{-1}.

6. Conclusions

Strong variations in natural radionuclides concentrations relate to differences in source material; soils have much higher Th and K contents, and lower U contents than weathered aplite, suggesting they were not completely formed in situ; many detrital minerals are inherited from other granitic source rocks, therefore, colluviation and slope movement may have been involved in the formation of these soils.

The highest U contents occur in the nodule with spheroidal weathering, especially in the core, and also in sand and clay fraction of residual clays of aplite. Higher concentration of U and Th in levels where clay fraction is more abundant, suggests that these elements are mainly adsorbed on clay minerals. This is consistent with limited U losses from the zone of the dyke during chemical weathering, and also with observations of significant Rn escape.

In the studied samples of aplite dyke the concentrations of uranium are 2–30 times higher than the Upper Continental Crust average, thus we may say that the aplite in Fornos de Algodres area is much enriched in this long-lived radionuclide, which decay products may emit high levels of ionizing radiation. Thus, aplite veins are potential source of elevated radon emission to the atmosphere that may have harmful environmental impact.

Acknowledgments

This work was conducted as part of the *Fundação para a Ciência e a Tecnologia* (FCT) funded postdoctoral program of M.J. Trindade (SFRH/BPD/41047/2007) and was supported by the FCT funded project PTDC/AAC-AMB/121375/2010.

References

Abdelouas, A., Lutze, W., Gong, W., Nuttall, E.H., Strietelmeier, B.A., Travis, B.J., 2000. Biological reduction of uranium in groundwater and subsurface soil. Sci. Total Environ. 250, 21–35.

Azevedo, M.R., Nolan, J., 1998. Hercynian late-post-tectonic granitic rocks from the Fornos de Algodres area (northern central Portugal). Lithos 44, 1–20.

Baeza, A., del Rio, M., Jimenez, A., Miro, C., Paniagua, J., 1995. Influence of geology and soil particle size on the surface area/volume activity ratio for natural radionuclides. J. Radioanal. Nucl. Chem. 189, 289–299.

Biscaye, P.E., 1965. Mineralogy and sedimentation of recent deep-sea clay in the Atlantic ocean and adjacent seas and oceans. Geol. Soc. Am. Bull. 76, 803–832.

Carvalho, F.P., Madruga, M.J., Reis, M.C., Alves, J.G., Oliveira, J.M., Gouveia, J., Silva, L., 2007. Radioactivity in the environment around past radium and uranium mining site of Portugal. J. Environ. Radioact. 96, 39–46.

Chan, L.S., Wong, P.W., Chen, Q.F., 2007. Abundances of radioelements (K, U, Th) in weathered igneous rocks in Hong Kong. J. Geophys. Eng. 4, 285–292.

De Corte, F., Vandenberghe, D., De Wispelaere, A., Buylaert, J.-P., Van den haute, P., 2006. Radon loss from encapsulated sediments in Ge gamma-ray spectrometry for the annual radiation dose determination in luminescence dating. Czech J. Phys. 56, D183–194.

Dias, M.I., Prudêncio, M.I., Gonçalves, M.A., Sequeira Braga, M.A., Gouveia, M.A., 2000. Geochemical and mineralogical diversity of clay materials in Fornos de Algodres region (Central Portugal) and its implications on provenance studies of ancient ceramics. In: Proceedings of the 1st Latin American Clay Conference, Funchal, Madeira, vol. 2, pp. 237–244.

Dias, M.I., Prudêncio, M.I., 2007. Neutron activation analysis of archaeological materials: an overview of the ITN NAA Laboratory, Portugal. Archaeometry 49, 383–393.

Dias, M.I., Prudêncio, M.I., 2008. On the importance of using scandium to normalize geochemical data preceding multivariate analyses applied to archaeometric pottery studies. Microchem. J. 88, 136–141.

Elles, P., Lee, S.Y., 2002. Radionuclide-contaminated soil: a mineralogical perspective for their remediation. In: Dixon, J.B., Schulze, D.G. (Eds.), Soil Mineralogy with Environmental Applications. Wisconsin Soil Sci. Soc. of America, Madison, pp. 737–763.

Ferreira, N., Iglesias Ponce de Léon, M., Noronha, F., Ribeiro, A., Ribeiro, M.L., 1987. Granitóides da Zona Centro Ibérica e seu enquadramento geodinâmico. In: Bea, F., Carnicero, A., Gonzalo, J.C., López Plaza, M., Rodriguez Alonso, M.D. (Eds.), Geologia de los Granitoides e Rocas asociadas del Macizo Hespérico. Editorial Rueda, Madrid, pp. 37–51.

Galhano, C., Rocha, F., Gomes, C., 1999. Geostatistical analysis of the influence of textural, mineralogical and geochemical parameters on the geotechnical behaviour of the "Clays Aveiro" formation (Portugal). Clay Miner. 34, 109–116.

Goinhas, J., 1987. Cadre géologique et métallogé-nique des ressources minières du Portugal. Chron. Rech. Min. 489, 25–42.

Gonçalves, L.S.M., Araújo, J.R.F., Fonseca, E.C., Pinto, M.C.S., Pinto, A.F.F., 1990. Carta Geológica de Portugal, Folha n° 17-B (Fornos de Algodres). LNEG – Laboratório de Geologia e Minas, Lisboa.

Gouveia, M.A., Prudêncio, M.I., 2000. New data on sixteen reference materials obtained by INAA. J. Radioanal. Nucl. Chem. 245, 105–108.

Govindaraju, K., 1994. Compilation of working values and sample description for 383 geostandards. Geostandards Newslett. 18.

Guibert, P., Lahaye, C., Bechtel, F., 2009. The importance of U-series disequilibrium of sediments in luminescence dating: a case study at the Roc de Marsal cave (Dordogne, France). Radiat. Meas. 44, 223–231.

Gusmão, C.C., 2008. Caracterização da radioactividade ambiente e contributo para análise de risco: Aplicação à área da antiga mina da Freixiosa. Universidade Nova de Lisboa, Tese de Mestrado, 127p.

Hall, I.R., McCave, N., 2000. Palaeocurrent reconstruction, sediment and thorium focussing on the Iberian margin over the last 140 ka. Earth Planet. Sci. Lett. 178, 151–164.

Martin-Pozas, J.M., 1968. El analisis mineralógico cuantitativo de los filosilicatos de la arcilla por difracción de rayos X. Tese de Doutoramento. Univ. Granada.

Matte, P., 1986. Tectonics and plate tectonic model for the Variscan belt of Europe. Tectonophysics 126, 329–374.

Murray, A.S., Aitken, M.J., 1988. Analysis of low-level naturally occurring radioactivity in small samples for use in thermoluminescence dating using high resolution gamma spectrometry. Int. J. Appl. Rad. Isot. 39, 145–158.

Neves, L.J.P.F., Pereira, A.J.S.C., Godinho, M.M., Dias, J.M., 1996. A radioactividade das rochas como factor de risco ambiental no território continental português. In: Borrego, C., Coelho, C., Arroja, L., Boia, C., Figueiredo, E. (Eds.), V Conferência Nacional sobre a Qualidade do Ambiente, vol. 1, pp. 641–649.

Oliveira, A., Rocha, F., Rodrigues, A., Jouanneau, J., Dias, A., Weber, O., Gomes, C., 2002. Clay minerals from the sedimentary cover from the northwest Iberian shelf. Prog. Oceanogr. 52, 233–247.

Pereira, A.J.S.C., Godinho, M.M., Neves, L.J.P.F., 2010. On the influence of faulting on small-scale soil–gas radon variability: a case study in the Iberian Uranium province. J. Environ. Radioact. 101, 875–882.

Perrin, J., Carrier, F., Guillot, L., 2006. Determination of the vertical distribution of radioelements (K, U, Th, Cs) in soils from portable HP-Ge spectrometer measurements: a tool for soil erosion studies. Appl. Radiat. Isot. 64, 830–843.

Pinto, M.S., Casquet, C., Ibarrola, E., Corretgé, L.G., Portugal Ferreira, M., 1987. Sıntese geocronológica dos granitóides do Maciço Hespérico. In: Bea, F., Carnicero, A., Gonzalo, J.C., López Plaza, M., Rodriguez Alonso, M.D. (Eds.), Geologia de los Granitoides e Rocas Asociadas del Macizo Hespérico. Editorial Rueda, Madrid, pp. 69–86.

Porcelli, D., Swarzenski, P.W., 2003. The behaviour of U- and Th-series nuclides in groundwater. Rev. Mineral. Geochem. 52, 317–361.

Reis, M.C., 2007. A Radioactividade no Ambiente. Gazeta de Fisica 30, 58–66.

Reynolds, B.C., Wasserburg, G.J., Baskaran, M., 2003. The transport of U- and Th-series nuclides in sandy confined aquifers. Geochim. Cosmochim. Acta 67, 1955–1972.

Ribeiro, A., Iglesias, M., Ribeiro, M.L., Pereira, E., 1983. Modèle geodynamique des Hercynides Ibériques. Com. Serv. Geol. Portugal LXIX, 291–294.

Richter, D., Zink, A., Przegietka, K., Cardoso, G.O., Gouveia, M.A., Prudêncio, M.I., 2003. Source calibrations and blind test results from the new Luminescence

Dating Laboratory at the Instituto Tecnológico e Nuclear, Sacavém, Portugal. Ancient TL 21, 1–7.
Rudnick, R.L., Gao, S., 2003. The composition of the continental crust. In: Holland, H.D., Turekian, K.K. (Eds.), Treatise Geochem.: The Crust, vol. 3. Elsevier, Oxford, pp. 1–64.
Salgado, L.M., Pereira, A.J.S.C., Neves, L.J.P.F., Godinho, M.M., 1998. Distribuição de U e Th em rochas da região de Tondela (Portugal Central). Comun. Inst. Geol. Mineiro 84, B122–B125.
Schultz, L.G., 1964. Quantitative interpretation of mineralogical composition X-ray and chemical data for the Pierre shale. U.S. Geol. Surv. Prof. Paper 391, 1–31.
Singh, J., Singh, H., Singh, S., Bajwa, B.S., Sonkawade, R.G., 2009. Comparative study of natural radioactivity levels in soil samples from the upper Siwaliks and Punjab, India using gamma-ray spectrometry. J. Environ. Radioact. 100, 94–98.
Taboada, T., Cortizas, A.M., Garcıa, C., Garcıa-Rodeja, E., 2006. Uranium and thorium in weathering and pedogenetic profiles developed on granitic rocks from NW Spain. Sci. Total Environ. 356, 192–206.
Thorez, J., 1976. Practical identification of clay minerals. G. Lelotte, Belgium.
Trindade, M.J., Dias, M.I., Prudêncio, M.I., Rocha, F., 2010. Urânio e outros elementos em argilas residuais de doleritos, granitos e aplito-pegmatitos da região de Fornos de Algodres, Beira Alta. Revista electrónica e-Terra 13, 1–4.
Trindade, M.J., Prudêncio, M.I., Burbidge, C.I., Dias, M.I., Cardoso, G., Marques, R., Rocha, F., 2013. Distribution of naturally occurring radionuclides (K, Th and U) in weathered rocks of various lithological types from the uranium bearing region of Fornos de Algodres, Portugal. In: Proceedings of the 2nd Luminescence in Archaeology International Symposia (L.A.I.S), special issue of Mediterranean Archaeology & Archaeometry.
Trindade, M.J., Prudêncio, M.I., Rocha, F., Dias, M.I., 2011. Variation of mineral and chemical composition, especially actinides and lanthanides, in size fractions of residual clays of dolerite and aplite dykes from central Portugal. In: Euroclay 2011. Book of Abstracts, Antalya, Turkey, pp. 33–34.
United Nations Scientific Committee on the Effects of Atomic Radiation (UNSCEAR), 1988. Sources and Effects of Ionizing Radiation. United Nations Scientific Committee on the Effects of Atomic Radiation, UN, New York.
Woodborne, S., Vogel, J.C., 1997. Luminescence dating at Rose Cottage cave: a progress report. S. Afr. J. Sci. 93, 467–470.